Cement and Concrete Research 40 (2010) 845–850

Contents lists available at ScienceDirect

Cement and Concrete Research

journal homepage: http://ees.elsevier.com/CEMCON/default.asp

Effect of pressure on early hydration of class H and white cement

George W. Scherer [a,*], Gary P. Funkhouser [b], S. Peethamparan [a,1]

[a] Princeton University, Civil & Env. Eng./PRISM, Eng. Quad. E-319, Princeton, NJ 08544, USA
[b] Halliburton, Duncan Technology Center, 2600 South 2nd Street, Duncan, OK 73536-0470, USA

ARTICLE INFO

Article history:
Received 21 September 2009
Accepted 25 January 2010

Keywords:
Hydration
Kinetics
Modeling
Rheology
Workability

ABSTRACT

The change in viscosity of cement slurry with temperature and pressure can be predicted by assuming that hydration can be treated as an activated process and that a given viscosity corresponds to a fixed degree of reaction. For Class H and White cements, chemical shrinkage experiments indicate that the activation energy is 33.8 kJ/mole and rheological measurements yield an activation volume of $-30\ cm^3$/mole. With these parameters, it is possible to predict the limit of pumpability of the slurry (which corresponds to a viscosity of about 2.5 Pa s) for arbitrary temperature and pressure cycles. This method of prediction requires that the physics of the process remain the same, but simply change in rate; therefore, the range of applicability is expected to be limited to temperatures below about 100 °C, since new phases occur at higher temperatures.

1. Introduction

The search for petroleum resources requires drilling to greater depths, where temperatures and pressures are so high (*viz.*, up to 200 °C and 150 MPa in deep wells) that they challenge the capabilities of construction materials used in the wells. In particular, sealing the steel casing into a well requires pumping of a cement slurry to the bottom of the well and forcing it to rise into the annular gap between the outside of the casing and the surrounding geological formation [1]. It is essential that the cement not set prematurely (which would require drilling it out, and would compromise the seal around the casing), nor take excessively long to set (which would cause expensive delays before drilling could resume). Therefore, it is important to be able to predict the influence of elevated temperature, T, and pressure, p, on the rheology of the cement slurry. In this work, we measure the rate of increase of slurry viscosity, η, over a range of T and p, and find that the change in η can be described by an activation energy and activation volume. It is then possible to predict quantitatively how the viscosity will change during an arbitrary variation in T and p. In the present study, we restrict the experiments to $T \leq 65$ °C, corresponding to well depths of ~1500 m, so the cement phases are those conventionally found at ambient temperature; future work must extend to higher temperatures where other phases occur [2].

To quantify the rheology of a cement slurry, the oil industry uses a device called a consistometer [3]. It consists of a rotating cup with a volume of about 0.475 l that is filled with slurry; the viscosity is determined from the torque exerted on a set of stationary paddles immersed in the slurry. Pressure is applied on the slurry via white mineral oil that fills the vessel; it is heated from the perimeter by elements in the annulus between the rotating cup and the wall of the pressure vessel. Consequently, the pressure response is immediate and spatially uniform, whereas the temperature response is slower and radial gradients of a few degrees are typical. The viscosity is reported in Bearden consistency units, which are linearly related to the torque, and therefore to the speed of rotation of the consistometer. Based on calibrations performed at Halliburton, for the type of instrument used in this study, the unit conversion is given by the following empirical correlation [4]:

$$\frac{\mathrm{Bc}}{\mathrm{Pa\cdot s}} \approx 10\left(\frac{\mathrm{RPM}}{50}\right)^{0.92} \tag{1}$$

where RPM = rotations per minute of the sample cup. For RPM = 150, as used in the present study, the viscosity in Bc is 27.5 times the viscosity in Pa s. The "limit of pumpability" (LOP) beyond which the slurry is too viscous to be forced around the casing is ~70–100 Bc, or $\eta \approx 2.5$ Pa s, which is roughly the viscosity of warm honey. Our goal is to predict the time at which the viscosity of the slurry reaches this level (LOP = 70 Bc).

2. Theory

Our basic assumption is that the viscosity of the slurry corresponds to a certain degree of hydration of the cement, so we need to be able to predict the influence of T and p on the rate of hydration. Several studies [*e.g.*, 5–9] have shown that the kinetics of this process are well

* Corresponding author.
E-mail address: scherer@princeton.edu (G.W. Scherer).
[1] Present address: Clarkson University, Civil & Env. Eng., 8 Clarkson Avenue, Potsdam, NY 13699, USA.

0008-8846/$ – see front matter © 2010 Elsevier Ltd. All rights reserved.
doi:10.1016/j.cemconres.2010.01.013

described by Avrami-type equations [10], which assume that the process involves nucleation and growth. A recent study of the chemical shrinkage kinetics of oil well cement [9] showed that the reaction was well described by the Avrami–Cahn model that was first applied to hydration by Thomas [8]. Cahn [11] extended Avrami's model, which assumes a random spatial distribution of nuclei [12], to the case where nucleation occurs on grain boundaries (as occurs in phase transformations in metals). Thomas argued that this model should also describe hydration, since the product nucleates on the surface of the cement grains. Indeed, the model provides a better fit to hydration kinetics of tricalcium silicate (C_3S)[2] [8] or cement [9] with fewer parameters than the conventional Avrami model.

The full expression of the Avrami–Cahn model is complicated, but when the degree of reaction is small, it reduces to [9]

$$X \approx \frac{\pi}{3} O_v^B I_B G^3 t^4 \tag{2}$$

where X is the volume fraction of the reactant transformed, O_v^B is the boundary area per unit volume, I_B is the nucleation rate on the boundary (events per unit area per time), and G is the linear growth rate of the product. Eq. (2) applies at constant T and p for a product that is spherical, and where I_B and G are constant. This simplified expression was found to describe chemical shrinkage kinetics of oil well cement over time periods exceeding the initial set, as identified by the Vicat needle test [9]. Since that point corresponds to a viscosity well in excess of the LOP, we can use Eq. (2) to predict the time, t_P, when the LOP is reached.

Before attempting to quantify the temperature and pressure dependence of the parameters in Eq. (2), we should consider the advantages and limitations of the model. The hydration of cement involves the reaction of water with several reactants (primarily tricalcium silicate, tricalcium aluminate, dicalcium silicate, gypsum) and precipitation of several products (including calcium–silicate–hydrate with uncertain stoichiometry, calcium hydroxide, ettringite and other sulfate minerals). It is obviously a gross simplification to describe this process in terms of a single nucleation and growth rate. To handle the true complexity of the process requires a far more sophisticated approach, such as the *HydratiCA* model being developed by Bullard [13,14]. However, our goal is to predict the change in rheology of the system, not to explain how the rheology depends on the interactions of the components. That is, we suppose that a certain level of viscosity corresponds to a certain degree of reaction of the products; if that is so, then we only need to find out how a change in T or p affects the time to reach that degree of reaction. Even if certain phases have a greater influence than others [15], it does not matter to us as long as the ensemble of phases does not change with T and p. Therefore we regard I_B and G as global parameters that describe the rate of formation of the ensemble of products. The validity of this approach can be judged by the quality of the resulting predictions.

To illustrate the dependence of the nucleation and growth processes on T, p, and composition, let us consider the dissolution of C_3S [16]

$$Ca_3SiO_5 + 3H_2O \rightleftharpoons 3Ca^{2+} + H_2SiO_4^{2-} + 4OH^- \tag{3}$$

and C–S–H with a Ca/Si ratio of 2:

$$C_2SH_7 \rightleftharpoons 2Ca^{2+} + H_2SiO_4^{2-} + 2OH^- + 5H_2O \tag{4}$$

The activity product, Q, of the latter compound is

$$Q = \left(a_{Ca^{2+}}^p\right)^2 a_{H_2SiO_4^{2-}}^p \left(a_{OH^-}^p\right)^2 \left(a_H^p\right)^5 \tag{5}$$

[2] We use conventional cement chemistry notation, *e.g.* C = CaO, S = SiO_2, H = H_2O.

where a_i^p is the activity of component i at pressure p. At the solubility limit, $Q = K$, so precipitation occurs when the solubility ratio,

$$S = \frac{Q}{K} \tag{6}$$

is greater than unity. The free energy driving precipitation is given by

$$\Delta\mu = -RT \ln(S) \tag{7}$$

Particles of C_3S dissolve according to Eq. (3), so that the concentration of those ions increases in the water adjacent to the particle. When the concentration is high enough so that $S > 1$, then it becomes possible for C–S–H to nucleate and grow. The rates of those processes increase with the magnitude of S.

The linear rate of growth, G, of a crystal is given by [10]

$$G = \Omega^{1/3} \nu(T,p) f(S) \left[1 - \exp\left(\frac{\Delta\mu}{RT}\right)\right] = \Omega^{1/3} \nu(T,p) f(S) \left(1 - \frac{1}{S}\right) \tag{8}$$

where Ω is the molecular volume, so $\Omega^{1/3}$ is a molecular dimension, ν is the frequency of jumps from the liquid onto the surface of the crystal, and f is an interface site factor (or accommodation coefficient) that represents the fraction of surface sites where attachment will be successful; the second equality is obtained by use of Eq. (7). If the surface is rough, then f is near unity; if the surface is smooth, then growth may occur by attachment of atoms at the edge of a screw dislocation or by nucleation of a disk of atoms that propagates laterally across the surface of the crystal. The dependence of G on S in these cases is discussed in the review by Nielsen [17].

The nucleation rate of a crystal from a solution is given by [10]

$$I_B = \frac{\nu(T,p)}{\Omega} \exp\left[-\frac{16\pi\Omega^2\gamma^3}{3(kT)^3 \ln^2(S)}\right] \tag{9}$$

where γ is the interfacial energy of the nucleus. It is reasonable to assume that ν has Arrhenius-type temperature dependence, but that would not apply to G and I_B in Eqs. (8) and (9), unless the supersaturation is so large (or the nucleation barriers are so small) that the rates of nucleation and growth are dominated by the interface attachment kinetics through ν. In that case, we can write

$$G(T,p) \approx G_0 \exp\left(-\frac{\Delta E_G^\ddagger + p\Delta V_G^\ddagger}{RT}\right) \equiv G_0 q_G(T,p) \tag{10}$$

where $\Delta E_G^\ddagger$ and $\Delta V_G^\ddagger$ are the activation energy and activation volume for growth, R is the ideal gas constant, and G_0 is a constant. Similarly,

$$I_B(T,p) \approx I_0 \exp\left(-\frac{\Delta E_I^\ddagger + p\Delta V_I^\ddagger}{RT}\right) \equiv I_0 q_I(T,p) \tag{11}$$

where $\Delta E_I^\ddagger$ and $\Delta V_I^\ddagger$ are the activation energy and activation volume for nucleation.

Using Eqs. (10) and (11) in Eq. (2), at constant T and p we obtain

$$X \approx \frac{\pi}{3} O_v^B I_0 G_0^3 \exp\left[-\frac{4\left(\Delta E^\ddagger + p\Delta V^\ddagger\right)}{RT}\right] t^4 \tag{12}$$

where

$$\Delta E^\ddagger = \frac{3\Delta E_G^\ddagger + \Delta E_I^\ddagger}{4} \tag{13}$$

and

$$\Delta V^\ddagger = \frac{3\Delta V_G^\ddagger + \Delta V_I^\ddagger}{4} \tag{14}$$

however, if T and p change with time, Eq. (2) must be replaced by [18]

$$X(t) = \frac{4\pi}{3}\int_0^t \left(\int_{t'}^t G\left[T\left(t''\right), p\left(t''\right)\right]dt''\right)^3 O_v^B I_B\left[T\left(t'\right), p\left(t'\right)\right]dt' \quad (15)$$

this means that the number of nuclei formed per unit volume between time t' and $t'+\mathrm{d}t'$ is $O_v^B I_B[T(t'), p(t')]\mathrm{d}t'$, and each of these grows at a time-dependent rate so that their radius, r, is described by the integral over G from the time of nucleation (t') until the current time, t. The volume of each particle is $4\pi r^3/3$, and the total amount of product produced by particles nucleated at time t' is equal to the number of those particles times their volume. The total amount of product is obtained by integrating over all nucleation times from 0 to t. To evaluate the amount of hydration when the pressure and temperature are increased in an arbitrary way, we must use Eqs. (10) and (11) in Eq. (15).

We find the time at which the LOP occurs, t_{LOP}, under ambient conditions from Eq. (12):

$$X_{LOP} \approx \frac{\pi}{3} O_v^B I_0 G_0^3 \exp\left[-\frac{4\left(\Delta E^{\ddagger} + p_0 \Delta V^{\ddagger}\right)}{RT_0}\right] t_{LOP}^4 \quad (16)$$

where T_0 and p_0 are ambient temperature and pressure, respectively. Assuming that the loss of pumpability corresponds to a fixed degree of reaction, X_{LOP} is not a function of T and p, so we can set Eq. (16) equal to the right side of Eq. (15). After canceling the constants, we obtain

$$\exp\left[-\frac{4\left(\Delta E^{\ddagger} + p_0 \Delta V^{\ddagger}\right)}{RT_0}\right] t_{LOP}^4(T_0, p_0) = 4\int_0^{t_{LOP}} \left(\int_{t'}^{t_{LOP}} q_G\left[T\left(t''\right), p\left(t''\right)\right]dt''\right)^3 q_I\left[T\left(t'\right), p\left(t'\right)\right]dt' \quad (17)$$

where the functions q_G and q_I are defined in Eqs. (10) and (11), respectively. If the activation energies and volumes are known, this equation can be evaluated for any thermal and pressure cycle to find t_{LOP}.

Many studies have investigated the temperature dependence of the rate of hydration, and found that it can be described by an Arrhenius equation with an effective activation energy, $\Delta E^{\ddagger}$, of about 35–40 kJ/mole [5–8,19–22]. Using the Avrami–Cahn model, it is possible to separate $\Delta E_G^{\ddagger}$ and $\Delta E_I^{\ddagger}$ [8]; we will use values obtained in that way at ambient pressure [9]. There has been comparatively less work done on the pressure effect on hydration. Some work addresses the effect of pressure on the structure of the product, rather than the rate of the reaction [23,24]. Several studies [25–27] have reported acceleration in the rate of hydration under pressure. Bresson *et al.* [28] found that pressures up to 100 MPa accelerated the rate of hydration (as reflected in the change of solution conductivity), and that the conductivity and degree of hydration were linearly related, independent of p (implying that the pressure did not change the nature of the reaction, only its rate). Similar conclusions were reached by Méducin *et al.* [29]. Jupe *et al.* [30] used synchrotron X-ray radiation to perform diffraction studies on cement hydrating within a pressure cell [31]. They found that the accelerating effect of pressure was diminished (at 180 °C) by the presence of some pozzolanic additives, but there were also changes in the nature of the products [32]. The effect of pressure on hydration kinetics reported in the literature [27,28,33] was successfully modeled by Lin and Meyer [34] using an empirical power law, rather than the activated state model used here.

3. Experimental procedure

The experiments were performed on Class H oil well cement (Lafarge) and White cement (Lehigh). The compositions are shown in Table 1. Quantitative X-ray diffraction patterns were obtained on a PANalytical X'Pert PRO diffractometer with a Cu Kα source and a scan interval of 5–50°. C_3S and C_2S were obtained from the whole-sample diffraction pattern. Sulfate-containing phases were determined after extraction of the silicate phases with maleic acid in methanol. Aluminate phases (C_3A and C_4AF), quartz, barite, calcite, dolomite, and periclase were determined after extraction of the sulfate phases with 10% ammonium chloride solution.

Table 1
Mineralogical composition of cement (wt.%).

Component	White cement (WPC)	Class H cement (OWC)
C_3S	61.86	63.98
C_2S	28.08	15.84
C_3A	4.13	0.57
C_4AF	0.09	11.33
Gypsum	0.06	1.81
Bassanite	1.41	0.76
Anhydrite	2.30	3.24
Syngenite	0.00	0.30
Ca-langbeinite	0.00	0.06
Gorgeyite	0.07	0.56
Quartz	0.22	0.24
Calcite	0.08	0.00
Dolomite	0.01	0.00
Periclase	0.01	1.32
Free lime	1.60	0.13
Barite	0.08	0.01
Arcanite	0.04	0.21
Total	100.04	100.31

The particle size distributions shown in Fig. 1 were measured by laser diffraction (Malvern Mastersizer 2000) with the sample suspended in isopropyl alcohol.

Cement slurries were prepared according to ANSI/API RP10B-2 [35] using 700 g of cement and either 266 g (for Class H, w/c = 0.38) or 322 g (for White cement, w/c = 0.46) of deionized water. Thickening times were measured on a Halliburton high-pressure, high-temperature consistometer with Chandler modifications for data acquisition.

Chemical shrinkage experiments were performed in a novel apparatus described in Ref. [36]. The experimental details and the analysis in terms of the Avrami–Cahn theory are described in Ref. [9]; only the results are presented here.

Two types of consistometer experiments were performed: (1) pressure jumps, in which the pressure was applied in <1.5 min and the temperature equilibrated in <7 min; (2) pressure ramps, in which T and p both increase linearly with time, arriving simultaneously (at

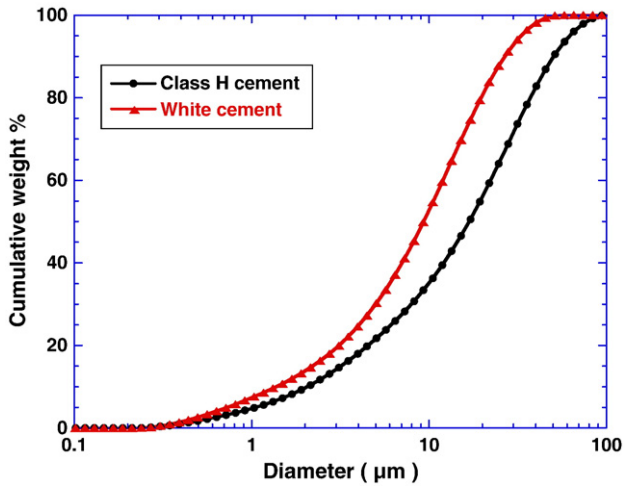

Fig. 1. Cumulative particle size distribution for Class H and White cements.

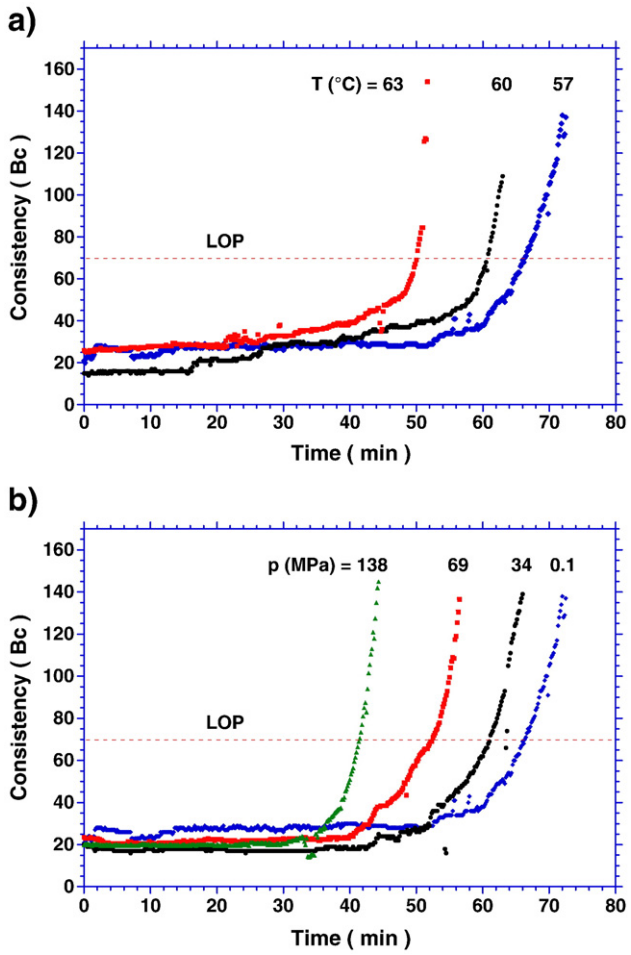

Fig. 2. Consistometer results for White cement during ramps over $\tau \approx 40$ min to the final values. (a) $p_0 = p_H = 0.1$ MPa, $T_0 = 27$ °C, T_H shown on curves; (b) $T_0 = 27$ °C, $p_0 = 0.1$ MPa, $T_H = 57$ °C, p_H shown on curves.

time $t = \tau$) at hold values (T_H and p_H). The latter experiments are described by

$$T(t) = \begin{cases} T_0 + \left(\frac{T_H - T_0}{\tau}\right)t & , 0 \le t \le \tau \\ T_H & , \tau < t \end{cases}$$
$$P(t) = \begin{cases} P_0 + \left(\frac{P_H - P_0}{\tau}\right)t & , 0 \le t \le \tau \\ P_H & , \tau < t \end{cases} \quad (18)$$

Class H Cement: Experiments of type (1) were performed at $T_0 \approx 27$ °C (80 °F) and $p_H = 0.1$, 34.5, 69.0, and 138 MPa. In one series of type (2) experiments, the temperature was ramped to 57 °C (135 °F) and the pressure was ramped to 34.5 MPa over periods of $\tau = 20$, 40, and 100 min. In other cases, T and p were both raised over $\tau = 40$ min.

White Cement: Only experiments of type (2) were performed, with ramp time of $\tau = 40$ min, $T_0 \approx 27$ °C and $p_H = 0.1$ MPa. Three series were run: (i) $T_H = T_0 \approx 27$ °C and $p_H = 0.1$, 34.5, 69.0, and 138 MPa; (ii) $T_H = 57$ °C and $p_H = 0.1$, 34.5, 69.0, and 138 MPa (see Fig. 2b); (iii) $p_H = 34.5$ MPa and $T_H = 57$, 60, and 63 °C (see Fig. 2a).

All of the LOP measurements were done in duplicate or triplicate. The maximum relative deviation between runs was less than 8% of the mean; however, most were within 2%. To avoid significant thermal lag in the consistometer, the minimum ramp time is 20 min for the temperatures used in these tests. The slurry temperature (measured with a Type J thermocouple in the hollow shaft of the paddle in the center of the slurry) responds quickly to the surrounding oil temperature with the rapid stirring rate. The temperature overshoots and returns to the set point temperature in about 12 min. Shorter ramp times result in higher overshoots, with a maximum of 2.2 °C overshoot on the 20 min ramp. Beyond this time, the temperature is controlled to within 0.5 °C of the set point until the slurry exceeds the pumpable consistency and the heat of hydration increases the slurry temperature. To avoid any complication from the time taken to achieve the final constant temperature in the consistometer, the activation energy was calculated from dilatometer experiments in a thermostatted bath at atmospheric pressure [9]. The activation volume was calculated from isothermal pressure jump experiments at 27 °C. By running the test isothermally, the large thermal mass was not an issue. Temperature calibration is performed monthly according to ISO 10426-2 using a NIST traceable reference.

4. Results

Fig. 2 shows consistometer curves for the White cement for ramp times of $\tau \approx 40$ min. As the temperature or pressure of the hold increases, the curves shift to shorter times and become steeper. The similarity in shape suggests that T and p have qualitatively similar effects on the kinetics, but do not change the mechanism of the reaction. To quantify the shift, we begin with the pressure jump experiments. If we assume that the LOP corresponds to a fixed degree of hydration for any cycle of T and p, then Eqs. (12) and (16) lead to the following relationship between t_{LOP} and p:

$$\ln\left[\frac{t_{LOP}(p, T_0)}{t_{LOP}(p_0, T_0)}\right] = \frac{(p - p_0)\Delta V^{\ddagger}}{RT_0} \quad (19)$$

This expression should be accurate as long as $\tau \ll t_{LOP}$, which is the case in the experiments of type (1). Taking t_{LOP} as the time when the consistometer curve reaches 70 Bc, we find that Eq. (19) provides a very good fit to the data, as indicated in Fig. 3. The slope of the line is -0.0122 MPa^{-1}, which indicates that the activation volume is $\Delta V^{\ddagger} = -3.04 \times 10^{-5}$ m^3/mole $= -30$ cm^3/mole ≈ -51 Å^3/molecule. This is about 1.7 times the volume of a molecule of water. These experiments do not permit an accurate distinction between the activation volumes for nucleation and growth, so for the following calculations we assume that $\Delta V_G^{\ddagger} = \Delta V_I^{\ddagger} = \Delta V^{\ddagger}$.

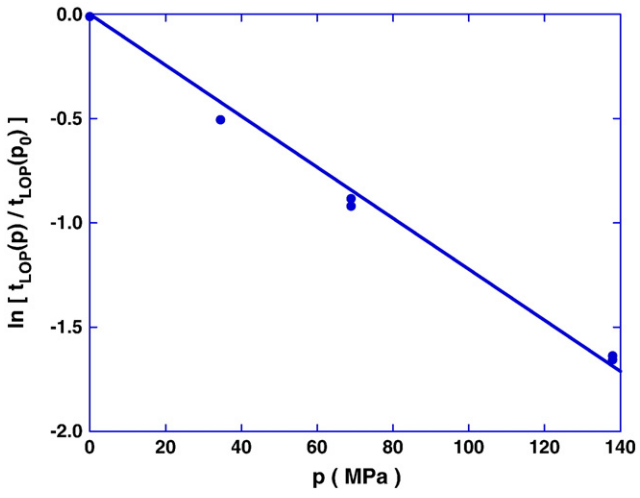

Fig. 3. Effect of hydrostatic pressure on time, t_{LOP}, to reach the limit of pumpability.

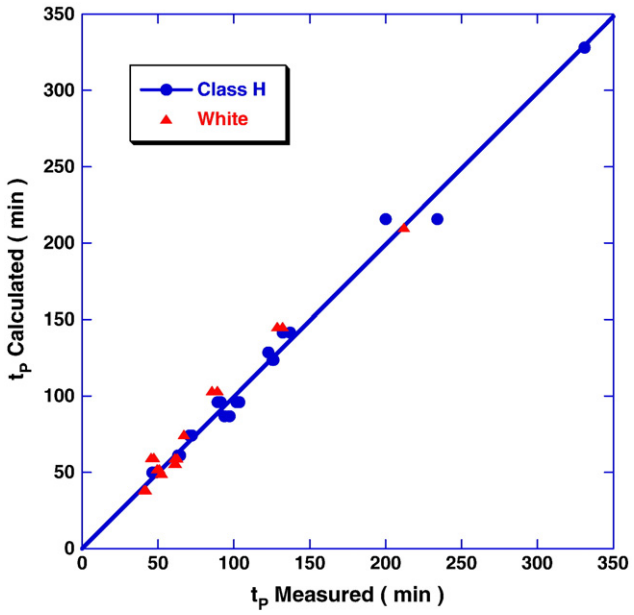

Fig. 4. Comparison of time until loss of pumpability calculated from Eqs. (17) and (18) versus measured values for Class H (circles) and White cement (triangles).

If the pressure is held at p_0, but the hydration is performed at a higher temperature, then the time to reach the LOP would be

$$\ln\left[\frac{t_{LOP}(p_0,T)}{t_{LOP}(p_0,T_0)}\right]=\frac{\Delta E^{\ddagger}+p_0\Delta V^{\ddagger}}{R}\left(\frac{1}{T}-\frac{1}{T_0}\right)\approx\frac{\Delta E^{\ddagger}}{R}\left(\frac{1}{T}-\frac{1}{T_0}\right) \tag{20}$$

where the second equality reflects the fact that the pressure term is negligible except far above ambient. Unfortunately, it is not possible to make temperature jump experiments, because of the large thermal mass of the consistometer, so we will make use of the activation energies obtained from chemical shrinkage measurements [9]. Applying the Avrami–Cahn model to those data yields $\Delta E_C^{\ddagger}\approx 38.5$ kJ/mole and $\Delta E_I^{\ddagger}\approx 19.5$ kJ/mole, so Eq. (13) gives $\Delta E^{\ddagger}\approx 33.8$ kJ/mole. We can use these values, together with the measured values of $\Delta V^{\ddagger}$ and t_{LOP}(27 °C, 0.1 MPa), to evaluate Eq. (17) with $T(t)$ and $p(t)$ given by Eq. (18) for the experiments of type (2), where $\tau\le t_{LOP}$. The comparison of the measured and calculated times for Class H and White cement is shown in Fig. 4, and the agreement is seen to be very good. The same activation energies and volumes were used for both materials.

Comparing Eqs. (19) and (20), we find that the pressure jump that would be equivalent to a temperature jump from T_0 to T would be

$$p-p_0\approx\frac{\Delta E^{\ddagger}}{\Delta V^{\ddagger}}\left(\frac{T_0-T}{T}\right) \tag{21}$$

For the cements studied here, for temperatures near ambient, Eq. (21) indicates a ratio of about 3.7 MPa/°C, so a small temperature change is equivalent to a rather large pressure increase, in terms of its effect on the rate of reaction.

5. Discussion

The activation parameters in Eqs. (10) and (11) describe the process of adding molecules to the product; that is, they reflect the energy barrier for a molecule to jump from the liquid onto the crystal. In the case of growth of crystals from the melt, the rate of this step is sometimes approximated as being proportional to the viscosity or diffusivity in the liquid. However, in the case of growth from solution, the attachment of ions onto the growing product can involve quite different motions and reactions. In particular, the activation energy for viscous flow in water is around 18 kJ/mole and the activation volume is near zero [37], which indicates much weaker dependence on T and p than is found for the hydration reaction. We have no information about the nature of the critical step in adding a molecule to the product, but the activated state formulation implies that a molecular complex is formed which then decomposes into the products. Growth is the reverse of dissolution, as in Eq. (4), so the same complex is expected to be involved in both processes. Forming that complex involves an activation energy, because bonds must be broken to construct it. The activation volume is the difference between the molar volumes of the complex and the reactants that create it; if the complex is denser, then the activation volume is negative, and applied pressure will favor its formation. This is an example of Le Chatelier's principle: the system responds to an increase in pressure by decreasing its volume (in this case, by reactants forming the denser activated complex). In the present situation, there are several simultaneous reactions, so we refer to "apparent" activation energies and volumes, which may reflect several simultaneous or sequential processes. The apparent activation volume is negative.

Since hydration results in chemical shrinkage, the application of pressure also changes the driving force for the reaction. Again according to Le Chatelier, pressure favors dissolution of the cement (*i.e.*, increase of K in Eq. (6)), because the reaction products occupy less volume than the reactants; therefore, the supersaturation ratio in Eqs. (6)–(9) changes with p. For example, it has been observed that the hydration reaction stops when the relative humidity drops below ~80%. That can be explained quantitatively as a result of the effect of (negative) pressure on the solubility of tricalcium silicate [38]. In that case, the activation volume is 2 or 3 times more negative (depending on the stoichiometry of the C–S–H formed) than what we find for the hydration reaction. This indicates that the effect of p on the rate of hydration (which is modest) is not primarily related to the change in S (which is large). As assumed above, it seems that the supersaturation is high enough under ambient conditions that any increase in S has a minor effect on the kinetics of hydration. Thus, we conclude that the pressure primarily accelerates setting through its effect on the kinetics, rather than its effect on the equilibrium solubility.

6. Conclusions

Although hydration of cement involves several chemical reactions, it is possible to make remarkably good predictions of the effects of temperature and pressure on the overall rate by treating hydration as a simply activated process. Moreover, the time to reach a certain value of slurry viscosity can be accurately predicted by assuming that the viscosity corresponds to a certain degree of reaction. This has been demonstrated here for the limit of pumpability and, in a companion study [9], the same approach has been shown to be equally valid for predicting the initial setting point. The success of this approach implies that increases in T and p change only the rate, not the nature, of the process. Bresson *et al.* [28] found that pressures up to 100 MPa changed the rate of hydration of C_3S, but did not alter the structure of the product. However, changes are expected at elevated temperatures. For example, it has been demonstrated [29] that C–S–H forms first at 200 °C and then converts to more stable crystalline phases. Presumably, a different set of parameters would be needed to predict the rate of change of the properties of the slurry when new phases begin to appear. The parameters presented in the present work have been tested to about 60 °C, but should not be expected to permit extrapolation above ~100 °C.

Acknowledgment

The authors thank Rocky Fitzgerald (Halliburton) for his assistance in conducting the thickening-time tests and Dale Bentz and Max Peltz (NIST) for the particle size analysis of the Class H cement. Financial

support from Halliburton for the research done at Princeton University is gratefully acknowledged.

References

[1] E.B. Nelson, D. Guillot (Eds.), Well Cementing, 2nd ed., Schlumberger, Sugar Land, Texas, 2006.
[2] H.F.W. Taylor, Cement Chemistry2nd ed., Thomas Telford, London, 1997.
[3] API Specification 10A/ISO 10426-1:2000.
[4] Dennis Gray, Halliburton, private communication.
[5] J.J. Thomas, H.M. Jennings, Effects of D_2O and mixing on the early hydration kinetics of tricalcium silicate, Chem. Mater. 11 (1999) 1907–1914.
[6] A.J. Allen, J.C. McLaughlin, D.A. Neumann, R.A. Livingston, In situ quasi-elastic scattering characterization of particle size effects on the hydration of tricalcium silicate, J. Mater. Res. 19 (11) (2004) 3242–3254.
[7] V.K. Peterson, D.A. Neumann, R.A. Livingston, Hydration of tricalcium and dicalcium silicate mixtures studied using quasielastic neutron scattering, J. Phys. Chem. B. 109 (2005) 14449–14453.
[8] J.J. Thomas, A new approach to modeling the nucleation and growth kinetics of tricalcium silicate hydration, J. Am. Ceram. Soc. 90 (10) (2007) 3282–3288.
[9] J. Zhang, S. Peethamparan, E.A. Weissinger, J. Vocaturo, G.W. Scherer, Early hydration and setting of oil well cement, submitted to CCR.
[10] J.W. Christian, The Theory of Transformations in Metals and Alloys, Part I, Pergamon, New York, 1975.
[11] J.W. Cahn, The kinetics of grain boundary nucleated reactions, Acta Metall. 4 (1956) 449–459.
[12] M. Avrami, Kinetics of phase change. II. Transformation–time relations for random distribution of nuclei, J. Chem. Phys. 8 (1940) 212–224.
[13] J.W. Bullard, A determination of hydration mechanisms for tricalcium silicate using a kinetic cellular automaton model, J. Am. Ceram. Soc. 91 (7) (2008) 2088–2097.
[14] J.W. Bullard, E. Enjolras, W.L. George, S.G. Satterfield, J.E. Terrill, A parallel reaction-transport model applied to cement hydration and microstructure development, Modelling Simul. Mater. Sci. Eng. 18 (2010) 025007 (16pp).
[15] C. Rössler, A. Eberhardt, H. Kučerová, B. Möser, Influence of hydration on the fluidity of normal Portland cement pastes, Cem. Concr. Res. 38 (7) (2008) 897–906.
[16] J.W. Bullard, R.J. Flatt, The role of calcium hydroxide precipitation in the kinetics of tricalcium silicate hydration, J. Am. Ceram. Soc (submitted).
[17] A.E. Nielsen, Electrolyte crystal growth mechanisms, J. Crystal Growth 67 (1984) 289–310.
[18] G.W. Scherer, Effect of inclusions on shrinkage, in: B.J.J. Zelinski, C.J. Brinker, D.E. Clark, D.R. Ulrich (Eds.), Better Ceramics through Chemistry IV, Mat. Res. Soc, Pittsburgh, PA, 1990, pp. 503–514.
[19] R.C.A. Pinto, K.C. Hover, Application of maturity approach to setting times, ACI Mater. J. 96 (1999) 686–691.
[20] P. Mounanga, V. Baroghel-Bouny, A. Loukili, A. Khelidj, Autogenous deformations of cement pastes: part I. Temperature effects at early age and micro–macro correlations, Cem. Concr. Res. 36 (2006) 110–122.
[21] J.L. Poole, K.A. Riding, K.J. Folliard, M.C.G. Juenger, A.K. Schindler, Methods for calculating activation energy for Portland cement, ACI Mater. J. 104 (2007) 303–311.
[22] K. Fujii, W. Kondo, Kinetics of the hydration of tricalcium silicate, J. Am. Ceram. Soc. 57 (11) (1974) 492–497.
[23] G. Le Saout, E. Lécolier, A. Rivereau, H. Zanni, Study of oilwell cements by solid-state NMR, C. R. Chimie 7 (2004) 383–388.
[24] G. Le Saout, E. Lécolier, A. Rivereau, H. Zanni, Chemical structure of cement aged at normal and elevated temperatures and pressures part I. Class G oilwell cement, Cem. Concr. Res. 36 (2006) 71–78.
[25] S.O. Oyefesobi, D.M. Roy, Hydrothermal studies of type V cement-quartz mixes, Cem. Concr. Res. 6 (1976) 803–810.
[26] A.A. Rahman, D.D. Double, Dilation of Portland cement grains during early hydration and the effect of applied hydrostatic pressure on hydration, Cem. Concr. Res. 12 (1982) 33–38.
[27] Q. Zhou, J.J. Beaudoin, Effect of applied hydrostatic stress on the hydration of Portland cement and C3S, Adv. Cem. Res. 15 (1) (2003) 9–16.
[28] B. Bresson, F. Meducin, H. Zanni, C. Noik, Hydration of tricalcium silicate (C3S) at high temperature and high pressure, J. Mater. Sci. 37 (2002) 5355–5365.
[29] F. Méducin, B. Bresson, N. Lequeux, M.-N. de Noirfontaine, H. Zanni, Calcium silicate hydrates investigated by solid-state high resolution ^{1}H and ^{29}Si nuclear magnetic resonance, Cem. Concr. Res. 37 (2007) 631–638.
[30] A.C. Jupe, A.P. Wilkinson, K. Luke, G.P. Funkhouser, Class H cement hydration at 180 °C and high pressure in the presence of added silica, Cem. Concr. Res. 38 (2008) 660–666.
[31] A.C. Jupe, A.P. Wilkinson, Sample cell for powder x-ray diffraction at up to 500 bars and 200 °C, Rev. Sci. Instr. 77 (2006) 113901-1–113901-4.
[32] A.C. Jupe, A.P. Wilkinson, K. Luke, G.P. Funkhouser, The Development and Utility of In-Situ Synchrotron Diffraction for Studying Oil Well Cement Hydration at Elevated Temperatures and Pressures, Proc. 2007 Int. Conf. Cement Chemistry, Montreal, 2007.
[33] M.E. Chenevert, B.K. Shrestha, Chemical shrinkage properties of oilfield cements, SPE Drilling Engineering 6 (1) (1991) 37–43.
[34] F. Lin, C. Meyer, Hydration kinetics modeling of Portland cement considering the effects of curing temperature and applied pressure, Cem. Concr. Res. 39 (2009) 255–265.
[35] Preparation of Slurry, Recommended Practice for Testing Well Cements, ANSI/API Recommended Practice 10B-2, 1st ed., American Petroleum Institute, Washington, DC, 2005, pp. 10–14.
[36] S. Peethamparan, E. Weissinger, J. Vocaturo, J. Zhang, and G.W. Scherer, Monitoring Chemical Shrinkage Using Pressure Sensors. Accepted for publication in ACI Special Proceedings CD on Material Science of Concrete, Spring Convention, Chicago, March 2010.
[37] K. Krynicki, C.D. Green, D.W. Sawyer, Pressure and temperature dependence of self-diffusion in water, Faraday Dis.. Chem. Soc. 66 (1978) 199–208.
[38] R.J. Flatt, G.W. Scherer, and J.W. Bullard, Why alite stops hydrating below 80% relative humidity, submitted to Cement Concr. Res.